Development 130, 1327-1337
S. Mackem, 2003 Published by The Company of Biologists Ltd
doi:10.1242/dev.00354

A role for the mesenchymal T-box gene *Brachyury* in AER formation during limb development

Chunqiao Liu*,‡, Eiichiro Nakamura‡, Vladimir Knezevic†, Sherrie Hunter, Katherine Thompson and Susan Mackem§

Laboratory of Pathology, Center for Cancer Research, NCI, NIH, Bethesda, MD 20892, USA
*Present address: Carnegie Inst Washington, Dept Embryol, Baltimore, MD 21210, USA
†Present address: 20/20 Gene Systems, Inc., Rockville, MD 20850, USA
‡These authors contributed equally to this work
§Author for correspondence (e-mail: smack@helix.nih.gov)

Accepted 18 December 2002

SUMMARY

During limb development, several signaling centers organize limb pattern. One of these, the apical ectodermal ridge (AER), is critical for proximodistal limb outgrowth mediated by FGFs. Signals from the underlying mesoderm, including WNTs and FGFs, regulate early steps of AER induction. Ectodermal factors, particularly *En1*, play a critical role in regulating morphogenesis of a mature, compact AER along the distal limb apex, from a broad ventral ectodermal precursor domain. Contribution of mesodermal factors to the morphogenesis of a mature AER is less clear. We previously noted that the chick *T* gene (*Brachyury*), the prototypical T-box transcription factor, is expressed in the limb bud as well as axial mesoderm and primitive streak. Here we show that *T* is expressed in lateral plate mesoderm at the onset of limb bud formation and subsequently in the subridge mesoderm beneath the AER. Retroviral misexpression of *T* in chick results in anterior extension of the AER and subsequent limb phenotypes consistent with augmented AER extent and function. Analysis of markers for functional AER in mouse $T^{-/-}$ null mutant limb buds reveals disrupted AER morphogenesis. Our data also suggest that FGF and WNT signals may operate both upstream and downstream of *T*. Taken together, the results show that *T* plays a role in the regulation of AER formation, particularly maturation, and suggest that *T* may also be a component of the epithelial-mesenchymal regulatory loop involved in maintenance of a mature functioning AER.

Key words: Brachyury, Limb development, AER formation, FGF, WNT

INTRODUCTION

The limb bud is induced in the lateral plate mesoderm in response to signals thought to be relayed in several steps from the embryo midline to the periphery (reviewed by Martin, 1998). Growth and patterning of the limb bud is organized by three signaling centers that arise before or soon after initial budding, and whose activities polarize pattern formation along the three axes of the limb: anteroposterior (AP), dorsoventral (DV), proximodistal (PD). Multiple cross-regulatory interactions between these signaling centers further coordinate development.

Limb outgrowth along the PD axis is regulated by FGF signals from a specialized columnar ectoderm that normally forms along the DV boundary at the limb apex, the apical ectodermal ridge (AER) (reviewed by Martin, 1998; Lewandoski et al., 2000; Moon and Capecchi, 2000; Sun et al., 2002). Interacting FGF and WNT cascades are critical in early limb induction, AER formation and reciprocal epithelial-mesenchymal interactions necessary for AER maintenance (reviewed by Martin, 1998; Tickle and Munsterberg, 2001). Several WNTs and FGFs, acting directly or indirectly, are able to induce ectopic limbs in the flank (e.g. Cohn et al., 1995; Ohuchi et al., 1997; Kawakami et al., 2001). Ultimately, FGF10 in the prospective limb lateral plate induces ectodermal *Wnt* (*Wnt3a* in chick) and *Fgf8* expression in the forming AER (Ohuchi et al., 1997; Kengaku et al., 1998; Galceran et al., 1999). FGF8 from the AER ectoderm also maintains high level *Fgf10* expression in limb mesoderm. Thus, reciprocal FGF8 and FGF10 signals form a positive regulatory loop by which AER and subridge mesoderm functionally maintain each other (Ohuchi et al., 1997; Revest et al., 2001). *Sonic hedgehog* (*Shh*), expressed in posterior limb bud mesoderm, regulates AP polarity and number of skeletal elements. Activation of *Shh* also depends on ridge signals and subsequently positive feedback between FGF4 from posterior ridge and SHH maintains both signaling centers (reviewed by Capdevila and Johnson, 2000).

AER induction, as well as later maturation, is normally closely linked to DV boundary formation although they can be uncoupled (reviewed by Zeller and Duboule, 1997; Tickle and Munsterberg, 2001). Early upstream BMP signaling regulates

both processes in parallel (Ahn et al., 2001; Pizette et al., 2001); contributing to AER induction by upregulating *Msx* genes and to establishing DV polarity by activating *En1* expression in ventral ectoderm. EN1 represses *Wnt7a* expression in ventral ectoderm (Loomis et al., 1996; Logan et al., 1997), while dorsal ectodermal WNT7a signals activate *Lmx1b* in the underlying mesoderm to regulate dorsal fates (Parr and McMahon, 1995; Riddle et al., 1995; Vogel et al., 1995; Cygan et al., 1997; Chen et al., 1998).

The murine AER forms from a broad zone of *Fgf8*-expressing ventral ectoderm in the prospective limb region, both by movement of pre-AER cells to the DV border and loss of AER-gene expression in remaining ventral cells, to form a sharply demarcated ridge during maturation (Kimmel et al., 2000) (reviewed by Tickle and Munsterberg, 2001). This process is also regulated by *En1* in the ventral ectoderm, via repressing *Wnt7a* and setting a ventral border for mature AER (Cygan et al., 1997; Loomis et al., 1998; Kimmel et al., 2000). Although the chick differs somewhat from mouse in that *Fgf8* expression is more restricted from its onset (Crossley et al., 1996), a pseudostratified, columnar AER also forms from a broader zone of flat ectodermal precursors that compact into a sharp ridge along the DV apex (Altabef et al., 1997; Michaud et al., 1997). Regulation of maturation is likely to be conserved in chick; for example, *En1* also affects AER formation (Laufer et al., 1997; Logan et al., 1997; Rodriguez-Estaban et al., 1997). The role of mesodermal signals in later morphogenesis of a mature AER is unclear. Disruption of mesodermal FGF10 signaling interferes with early stages of AER induction, obscuring later function (Min et al., 1998; Xu et al., 1998; Arman et al., 1999; Sekine et al., 1999; Revest et al., 2001).

We previously noted expression of *Brachyury* (*T*) in early limb buds on northern blots (Knezevic et al., 1997a). *T* is the founding member of the T-box family of transcription factors which share a conserved DNA binding domain and play multiple roles during development (reviewed by Papaioannou and Silver, 1998), several of which are expressed in developing limb (Gibson-Brown et al., 1996; Gibson-Brown et al., 1998; Isaac et al., 1998; Logan et al., 1998; Ohuchi et al., 1998). *T* plays an essential role in primary mesoderm formation (reviewed by Herrmann, 1995) and has been implicated in both WNT and FGF signaling pathways during gastrulation (Smith et al., 1997; Yamaguchi et al., 1999a; Arnold et al., 2000; Tada and Smith, 2000; Galceran et al., 2001), but has not been reported to be expressed elsewhere. We found that *T* is expressed at low levels in lateral plate at the onset of limb initiation and persists in the subridge mesoderm of the limb bud, as well as several other sites associated with WNT and FGF signaling. Retroviral misexpression of *T* in chick causes anterior AER extension along the limb apex and skeletal phenotypes consistent with extended AER function, whereas loss of *T* in mutant mouse embryos disrupts normal AER morphogenesis. These results suggest *T* functions in the mesoderm to direct AER maturation along the DV limb border. Taken together, altered subridge *Fgf10* expression levels in response to in vivo changes in *T* expression, and the ability of ridge-specific WNT and FGF signals to induce *T* in vitro suggest that *T* may also regulate maintenance of a mature AER as a component of the reciprocal epithelial-mesenchymal signaling mediated by FGF and WNT pathways.

MATERIALS AND METHODS

Embryo isolation

White leghorn chicken eggs (Truslow Farms) were incubated at 38.5°C and staged according to Hamburger and Hamilton (Hamburger and Hamilton, 1951). The mouse $T^{+/-}$ mutant line T^{2J} (in C57BL6), containing a ~80 kb genomic deletion including the entire *T* gene (Herrmann et al., 1990), was obtained from the Jackson Laboratory. Extended survival of $T^{-/-}$ embryos (to ~E10.5) was achieved by breeding T^{2J}/C57BL6 line to wild-type FVB/N. $T^{-/-}$ embryos were easily identified phenotypically. Noon on the day of the appearance of the vaginal plug was considered E0.5.

In situ hybridization and immunostaining

Conditions for probe preparation and in situ hybridization were as previously described (Knezevic et al., 1997a; Knezevic et al., 1997b). For chick *T* probe, the color reaction contained 10% polyvinyl alcohol (Barth and Ivarie, 1994) to enhance detection sensitivity, and was developed for 12-18 hours. Other chick probes used included *Fgf4* (L. Niswander), *Fgf8* (J.-C. Izpisua-Belmonte), *Fgf10* (S. Noji), *Shh* (R. Riddle), and *Wnt5a* (T. Nohno). Mouse probes used included *Bmp4* (B. Hogan), *Fgf8* (G. Martin), *Fgf10* (D. Ornitz), *En1* (A. Joyner), *Lmx1b* (R. Johnson), *Msx1*, *Msx2* (R. Maas) and *Shh*, *Wnt7a* (A. McMahon). Whole-mount embryos were paraffin embedded or frozen in OCT and sectioned at 5-10 μm, or embedded in 3% agarose to cut 50 μm vibratome sections. Immunostaining of cryosections or paraffin sections (after antigen retrieval by steaming) was detected with peroxidase-linked secondary antibodies and Vectastain kit. Affinity purified DLX-antibody was a gift from G. Panganiban (for details, see Panganiban et al., 1997).

Proliferation and apoptosis assays

Mitosis-specific anti-phospho-histone H3 (Upstate Biotechnology) was used to immunostain multiple sections. Mitotic cells in equal-sized areas were counted and averaged for comparisons. Apoptosis was assessed on sections by TUNEL assay (Apoptag kit, Intergen) using fluoro-dNTP incorporation and direct fluorescence microscopy with propidium iodide counterstaining, or by whole-mount staining of fresh embryos with 1/50,000 Nile Blue sulfate in PBS.

Retrovirus preparation, infection and misexpression analysis

The chick *T* coding region (Knezevic et al., 1997a) was cloned as an *Nco*I-*Ear*I fragment into the *Nco*I-*Sma*I sites of Cla12Nco vector, and transferred into RCASBP as a *Cla*I fragment. Virus production and infection were as described by Morgan and Fekete (Morgan and Fekete, 1996), except that a Picospritzer II (Parker instruments) was used for injection. Parallel control infections with alkaline phosphatase (AP)-expressing virus (a gift from B. Morgan) were done to assess phenotype specificity, and adequacy of hindlimb infection by AP staining. *T*-virus infected embryos were also hybridized with a *T* probe as a control to evaluate adequacy of infection. Overall, 55-75% of *T*-infected embryos at early or late times post-infection had abnormalities. The extents of viral *T* expression in hindlimb suggested that the lack of visible effect of infection in the remaining embryos was due to inherent variability in infection spread (data not shown). Variability in amplification of *T*-virus also occurred in cell culture. For skeletal analysis, infected day 9-10 embryos were fixed in 5% TCA, stained with 0.1% Alcian Green 2GX in acid-alcohol, washed and dehydrated in absolute alcohol, and cleared in methyl salicylate.

T-antibody production, purification and analysis

T/GST fusion protein from plasmid expressing N-terminal (amino acids 1-123) T/GST fusion protein (a gift from B. Herrmann) was used to immunize rabbits using standard techniques. Antibody was affinity purified as described (Kispert and Herrmann, 1993). Protein extracts were prepared from dissected embryonic tissues by lysis in PBS

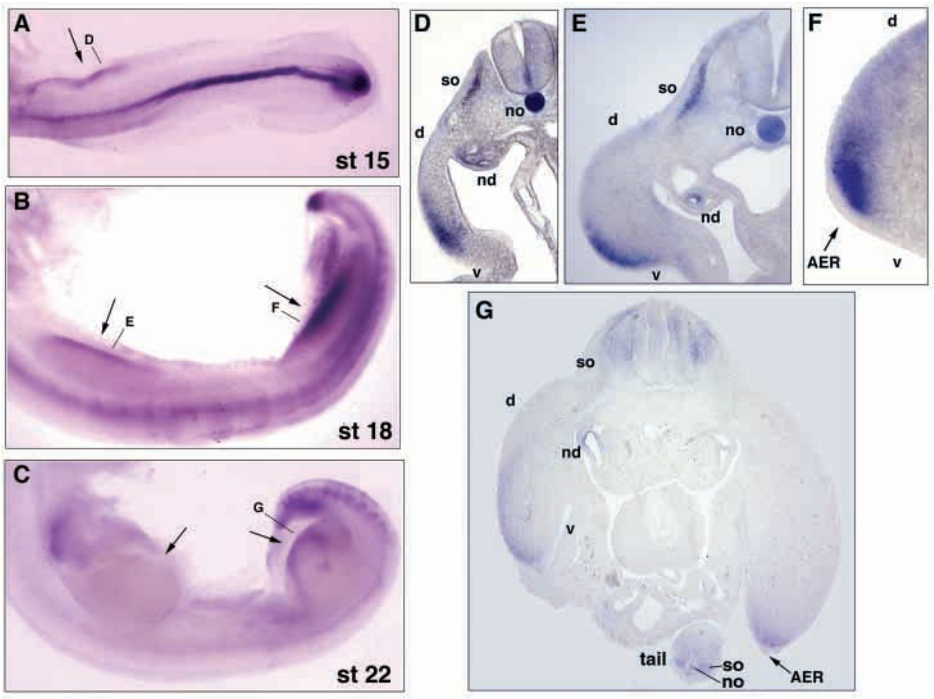

Fig. 1. Expression of *T* during limb development in chick. Whole-mount in situ hybridization with chick *T* probe. (A) *T* expression in lateral plate of the wing region at stage 15 (arrow), as well as weak expression in adjacent somites, and strong expression in notochord and tail bud. (B) At stage 18, *T* is expressed in a narrow strip of distal mesoderm underlying both wing and leg AER (arrows), as well as in somites, notochord and tail bud. (C) By stage 22, *T* expression is beginning to decline in wing, but is still very evident in leg bud (arrows). (D) Transverse section through wing region of a stage 15 embryo (as indicated in A) showing strong *T* expression in notochord (no), weak to moderate expression in wing lateral plate, somite (so) and nephric/Wolffian ducts (nd). (E,F) Transverse sections through wing (E) and leg (F) buds from a stage 18 embryo (as indicated in B), and (G) transverse section through leg bud of a stage 22 embryo (as indicated in C) showing *T* expression in the immediate subridge mesoderm beneath the AER (arrow) and continued weak expression in dermomyotome of somites (so) and in nephric ducts (nd). Note *T* expression is also seen in tail epithelial somites, at stage 22 (G). Signal development time was extended to visualize sites with weak expression (lateral plate, somites, limb bud). d, dorsal; v, ventral.

containing protease inhibitor cocktail, 10 μg/ml AEBSF, 1% SDS, and 0.5 mM DTT. Proteins, electrophoresed on 4-12% NuPAGE gradient gels (Novex), were blotted and probed with antibody using standard techniques. Monoclonal anti-α-tubulin (Sigma) served as an internal protein loading control. For immunohistochemistry, affinity-purified anti-T was pre-incubated with blotted 100 kDa protein (24 hours) to remove cross-reacting epitopes.

Chick limb mesenchyme cell culture and northern analysis

Primary cell cultures from stage 19-20 chick limb buds, as described (Knezevic et al., 1997b), were incubated with recombinant FGF4 (a gift from Genetics Institute, Inc.) or FGF8b (R&D systems) at 750 ng/ml and heparin sulphate (100 ng/ml). Cultures infected with *Wnt3a*-expressing retrovirus (a gift from Cliff Tabin) at a multiplicity of 3-5 IU/cell, were compared to RCASBP control. Northern analysis with chick *T* 3′UTR and control probes was as described previously (Knezevic et al., 1997a).

RESULTS

Expression of *T* during limb development

We previously detected chick *T* transcripts in limb buds by northern analysis (stages 20-24) (Knezevic et al., 1997a), and therefore evaluated the expression pattern by in situ hybridization. Weak expression of *T* in the prospective forelimb lateral plate and adjacent somites was first detected at about stage 15 (Fig. 1A,D). Subsequently, expression in forelimb and hindlimb bud increased (Fig. 1B) and localized to a thin strip of distal mesenchyme just beneath the AER (Fig. 1E,F). Weak expression was also seen in somitic dermomyotome and in Wolffian/nephric ducts (Fig. 1D,E). Expression waned by stage 22/23 in limb buds and adjacent somites (Fig. 1C,G) and became undetectable by stage 26-27 (not shown). Surprisingly, hybridization with a sense probe revealed antisense *T* transcripts at several sites including somites and limb buds (data not shown).

T protein expression in limb was verified with immunoblots of protein from different chick and mouse tissues, probed with affinity-purified anti-T. T protein was detected in early stage chick and mouse limb buds, albeit at much lower levels than tailbud (Fig. 2A). A highly abundant, cross-reacting, ubiquitous 100 kDa protein (see Fig. 2A) hampered in situ immunostaining even after affinity purification, necessitating extensive pre-adsorption against blotted 100 kDa proteins to deplete cross-reacting epitopes. Depleted antibody revealed mouse T protein in subridge limb mesoderm and somites, as in chick (Fig. 2B). The intriguing proximity of *T* expression to the forming AER was investigated using retroviral misexpression to perturb *T* in developing limb.

T misexpression causes anterior AER extension and ensuing late phenotypes

The prospective hindlimb lateral plate of stage 9-11 chick embryos was infected with RCASBP retrovirus expressing full-length T protein. Changes in limb bud morphology were discernible by stage 19-20 (~48 hours post-infection). The AER, visualized by *Fgf8* expression as a functional marker, extended farther anteriorly along the DV edge of infected limb buds, accompanied by variable broadening of the anterior limb bud (50%, 7/15, Fig. 3A,B). In some embryos, the ‘extended’ AER was widened and irregular (e.g. see Fig. 3B), but truly ectopic AERs away from the DV limb margin were not seen, except for rare, small isolated spots of *Fgf8* expression (data not shown). Older infected embryos (stage 24, ~60 hours post-

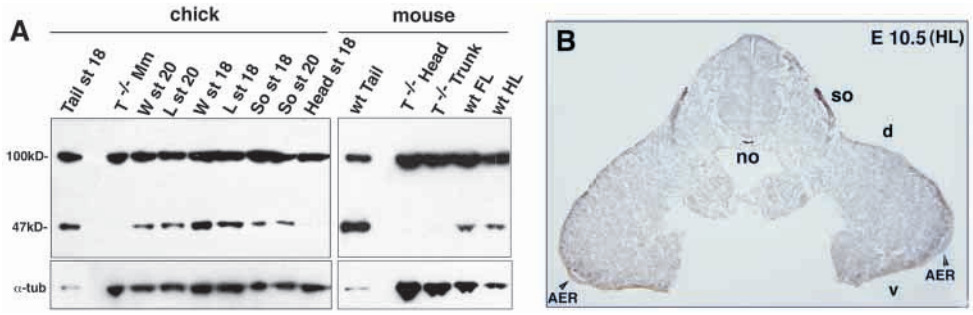

Fig. 2. Tissue distribution of T protein in limb bud stage chick and mouse embryos. (A) Western analysis of T protein in dissected tissues using affinity-purified polyclonal antibody. T protein (47 kDa band) was detected in chick wing (W) and leg (L) buds and in somites (So) at stages (st) 18 and 20, as well as in wild-type (wt) E10 mouse forelimb (FL) and hindlimb (HL) buds. No T protein band was detected in head or trunk (including forelimb buds) from $T^{-/-}$ mouse embryos (negative control). Chick or mouse tailbud protein was loaded as a positive control. A ubiquitous 100 kDa protein was recognized by affinity-purified T antibody in every tissue evaluated. Protein loading was assessed by reprobing blots with α-tubulin antibody (bottom). (B) Immunohistochemical detection of T protein in transverse hindlimb section of E10.5 mouse embryo, showing expression in notochord (no) somitic dermomyotome (so) and limb mesoderm subjacent to AER. Affinity purified antibody was exhaustively pre-adsorbed against 100 kDa proteins prior to use. d, dorsal; v, ventral.

infection) also had anteriorly extended AERs (40%, 12/29, Fig. 3C) and some embryos without extension still showed stronger *Fgf8* expression in the AER on the infected side (20%, 6/29 embryos, not shown), which may correlate with mild soft tissue phenotypes seen at day 10 (see below), perhaps reflecting later infection onset or spread. *Fgf4* expression, normally restricted to posterior AER, was also extended anteriorly in *T* infected limb buds (52%, 16/31, Fig. 3D), consistent with expanded AER extent and function.

At 10 days, *T*-infected embryos showed skeletal and soft tissue phenotypes predicted by earlier AER changes (75%, 21/28; no abnormalities in control-virus infections, 0/15). Skeletal abnormalities (54%, 15/28) included anterior digit duplications (Fig. 4B-D), in some cases with posterior transformation of anterior digits (Fig. 4B). Sometimes the anterior-most metatarsal was also thickened (Fig. 4C) or duplicated (Fig. 4D). The proportion of infected embryos with anterior digit changes correlated well with the incidence of anterior AER extension at earlier stages. SHH plays a central role regulating AP digit patterning and is often a factor in the production of anterior polydactyly (discussed in Knezevic et al., 1997b). Moreover, changes in AER extent might also be associated with ectopic *Shh* expression, driven by increased FGFs (reviewed by Martin, 1998). However, no ectopic anterior *Shh* was detected in a set of infected limb buds showing clear anterior broadening and AER extension (0/11, Fig. 3C). This may not be surprising since augmented AER function is not invariably linked to ectopic *Shh* induction (e.g. Pizette and Niswander, 1999; Zhang et al., 2000) and digit I specification does not require SHH (see Lewis et al., 2001).

T misexpression caused milder interdigital soft tissue changes in some embryos (21%, 6/28), including soft tissue broadening (Fig. 4E,F), delayed loss of webbing (Fig. 4E) and ectopic cartilage condensations (Fig. 4D,E). Inhibition of AER regression is associated with interdigital soft tissue overgrowth, apparently due to prolonged *Fgf8* expression in the AER at late stages (Pizette and Niswander, 1999). Stronger late *Fgf8* expression seen in some *T*-infected embryos may have a similar effect, suggesting *T* may delay AER regression.

Relationship of *T* to FGF and WNT signaling in limb

T is a transcription factor so we expected direct targets to be expressed in the mesoderm, where *T* is normally expressed, and to include secreted signals that regulate the AER. Since

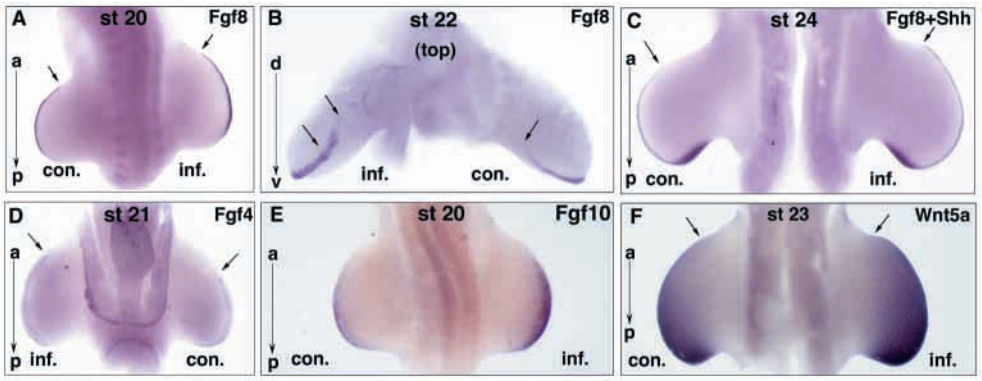

Fig. 3. Retroviral misexpression of *T* in prospective hindlimb causes anterior extension of the AER and early changes in *Fgf10* expression. All panels show dorsal side of embryos except B, which is viewed from the top (craniad) down and D, which shows a ventral view. The anteroposterior (a-p) or dorsoventral (d-v) orientations are indicated to left. (A-C) *Fgf8* expression in infected embryos harvested at stages 20 (A), 22 (B), and 24 (C). The embryo in C was also hybridized with a *Shh* probe. Broadening of the anterior limb bud on the infected (inf.) side compared to the contralateral control (con.) side was always accompanied by anterior extension of *Fgf8* expression in AER (arrows). No ectopic *Shh* expression was seen in the context of AER extension (C). (D) *Fgf4* expression in infected embryo at stage 21 showing expression has extended anteriorly in the AER on the infected side (arrows). (E) *Fgf10* expression in infected embryos at stage 20 was stronger and more extensive in the distal subridge mesoderm on the infected side. Color development times for *Fgf10* probe were kept very short to visualize mainly the distal mesoderm and prevent signal saturation. (F) *Wnt5a* expression was only slightly increased by stage 23 on the infected side (arrows), but showed no expression difference at earlier stages following infection (data not shown).

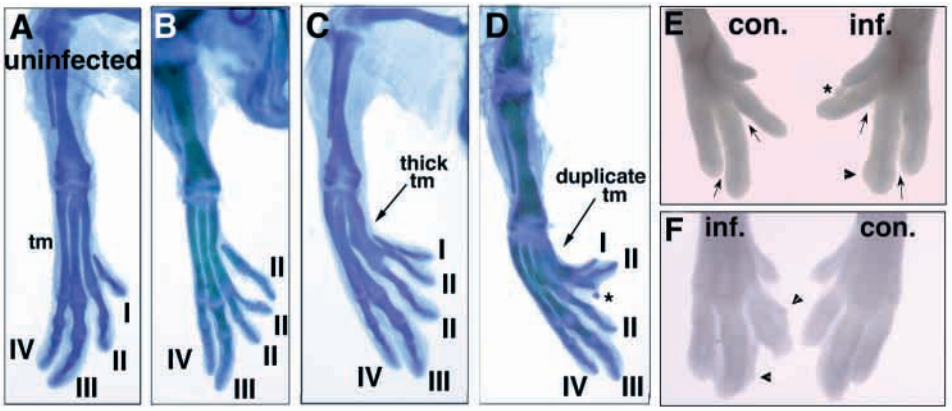

Fig. 4. Skeletal and soft tissue phenotypes due to retroviral misexpression of *T*. (A-D) Embryos harvested at day 9-10 were stained for cartilage. (A) Uninfected control leg with tarso-metatarsals (tm) and digits I-IV (anterior to posterior order) indicated. Digit identity was based on the number of phalangeal elements (1-4 for I-IV respectively). Skeletal phenotypes in infected legs (B-D) included partial (C) or complete (B,D) anterior digit duplications, and occasionally thickening (arrow, C) or duplication (arrow, D) of anterior tarsometatarsals. Some infected embryos at day 9-10 also showed changes in digital soft tissues in the infected (inf.) compared to contralateral control (con.) leg (panels E,F). These included digital soft tissue broadening (E,F arrowheads), ectopic cartilage condensations (D,E asterisk), and delayed loss of interdigital webbing (E, compare arrows). E, ventral side; F, dorsal side shown.

Wnts and *Fgfs* are *T* targets during gastrulation (Smith et al., 1997; Tada and Smith, 2000), we checked *Fgf10* and *Wnt5a*, both expressed in early distal limb mesenchyme. *Fgf10*, which regulates limb initiation and AER formation (Ohuchi et al., 1997; Min et al., 1998; Sekine et al., 1999), was increased in the distal subridge mesoderm in *T*-infected limb buds (7/14 total, stage 19-24) and was already upregulated by stage 19-20 (4/7 embryos, Fig. 3E), suggesting that *Fgf10* may be an early target of *T* in the subridge zone. *Wnt5a*, which plays a role in limb outgrowth (Yamaguchi et al., 1999b), was unchanged in stage 19-21 infected embryos (0/8, data not shown) and later was expanded slightly anteriorly (4/8, Fig. 3F), most likely as a very indirect effect.

Prominent *T* expression in apical subridge mesoderm suggested regulation by AER signals. FGFs and WNTs also function upstream of *T* during gastrulation (Smith et al., 1997; Yamaguchi et al., 1999a; Arnold et al., 2000; Galceran et al., 2001), so AER-specific WNTs and FGFs were tested. Since limb *T* expression was very weak, we evaluated quantitative effects on *T* expression in primary cultures of stage 19/20 limb mesenchyme. *T* was induced within 18 hours after infection with a *Wnt3a*-expressing virus (Fig. 5). Recombinant FGF8b induced *T* within 8 hours (Fig. 5), while recombinant FGF4 protein had no effect early or later (data not shown). Hence, both FGF8b and WNT3a ridge signals may participate in activating or maintaining subridge *T* expression. *Fgf4*, expressed in posterior AER, functionally overlaps with *Fgf8* (Sun et al., 2002) but shows some differences in receptor binding (Ornitz et al., 1996) and ability to regulate mesodermal genes (e.g. Haramis et al., 1995; Mahmood et al., 1995; Kimura et al., 2000), perhaps explaining its failure to induce *T*.

Disrupted AER formation in mouse $T^{-/-}$ embryos

To assess whether *T* plays a role in normal AER formation, we analyzed mouse $T^{-/-}$ embryos. The $T^{-/-}$ null mutant is an early embryonic lethal (~E10.5), precluding skeletal analysis, but allowing evaluation of forelimb AER formation. No hindlimb bud forms owing to disrupted posterior mesoderm formation and ensuing posterior truncations. $T^{-/-}$ forelimb buds were smaller than wild type and often more rounded at mature AER stages, lacking a sharp DV edge (see Figs 6, 7).

From its onset at E9, *Fgf8* expression in pre-AER ectoderm was mottled and weaker in $T^{-/-}$ embryos (Fig. 6A). Later, *Fgf8* continued to be irregular in the $T^{-/-}$ pre-AER, revealing its failure to compact normally toward the DV apex (Fig. 6B-E). At more mature stages (E9.75-10) the $T^{-/-}$ AER was wavy, zigzagging into both dorsal and ventral ectoderm, with variably weaker *Fgf8* levels (Fig. 6D,E). AER morphology was assessed with anti-DLX, since *Dlx* gene expression marks AER progenitors similarly to *Fgf8* (Panganiban et al., 1997; Loomis et al., 1998). DLX expression during AER morphogenesis (Fig. 7A-H′) was irregular and sometimes less clearly restricted to ventral ectoderm in $T^{-/-}$ embryos (e.g. Fig. 7C,D), and revealed that progression to a highly compact, pseudostratified AER

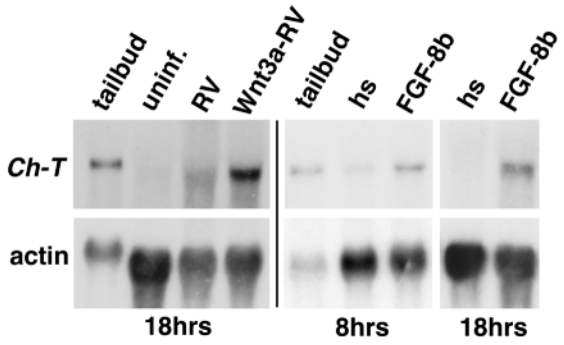

Fig. 5. WNT3a and FGF8b induce *T* expression in primary limb mesenchyme culture. Mesenchymal cells were dissociated from stage 19/20 chick embryo limb buds and used immediately. RNA from cells infected with *Wnt3a*-expressing retrovirus (Wnt3a-RV), control viral vector (RV), uninfected control (uninf.) or after treatment with either heparin sulphate (hs) alone or with recombinant FGF8b+hs (FGF-8b) were harvested at times indicated and hybridized with a chick *T* 3′-UTR probe (Ch-T), followed by a chick β-actin probe to control for loading. RNA extracted from stage 18 chick tail bud was included as a positive control. Both WNT3a and FGF8b induced *T* expression within 18 hours and activation by FGF8b protein was detectable by 8 hours. FGF4 protein had no effect on *T* expression at either time (data not shown).

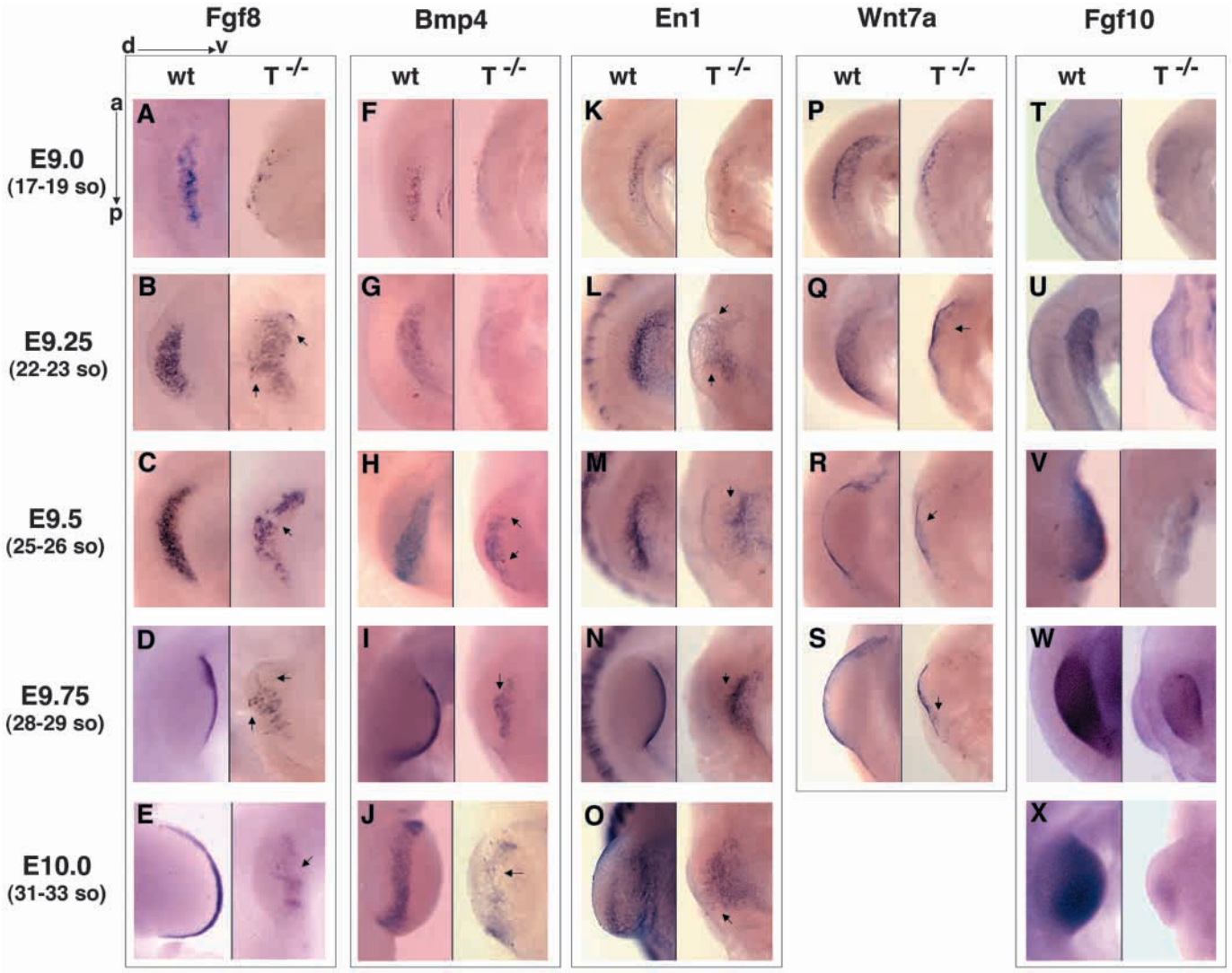

Fig. 6. Disrupted AER maturation and reduced *Fgf10* expression in $T^{-/-}$ embryos. Comparison of *Fgf8* (A-E), *Bmp4* (F-J), *En1* (K-O), *Wnt7a* (P-S) and *Fgf10* (T-X) expression in wild-type (wt, left sides) and $T^{-/-}$ (right sides) embryos at different stages as indicated to the left of each row by age and average somite (so) number in wild type. As indicated in the upper left corner, limb buds shown in each panel are oriented with dorsal to ventral axis (d→v) from left to right, and with anterior to posterior axis (a→p) from top to bottom of the panel. The small arrows highlight some of the focal gaps, irregularities, and wavy borders in pre-AER or AER zone revealed by marker expression patterns in $T^{-/-}$ limb buds. Note that $T^{-/-}$ embryos showed mottled early pre-AER expression (A,F) and later broad, weak, and irregular patterns of AER markers compared to very sharply demarcated expression in the wild type. *Fgf10* expression was substantially decreased by E9.5 and later (V-X). Note some $T^{-/-}$ limb buds were very irregularly shaped (eg. Q,T,V). Hybridization signals at various expression sites unaffected by loss of *T* (e.g. craniofacial, branchial arch, gut) were similar in $T^{-/-}$ and wild-type embryos, serving as internal controls (data not shown).

was delayed and erratic. Even in late stage $T^{-/-}$ limb buds with the mildest phenotype, the extent of AER maturation varied dramatically in neighboring sections (e.g. Fig. 7H vs H′).

Bmp4 is highly expressed in AER progenitors and BMP signalling has been implicated in AER induction and DV patterning (Ahn et al., 2001; Pizette et al., 2001). *Bmp4* expression in $T^{-/-}$ embryos was altered in parallel with *Fgf8*, starting weak and patchy at E9 (Fig. 6F), and remaining broad and irregular at later stages (Fig. 6G-J), consistent with abnormal AER maturation. Since *Bmp4* is expressed in ectoderm and in mesenchyme, the distribution was examined on sections, revealing abnormalities in AER morphogenesis similar to those seen with DLX antibody (Fig. 7I-N). Mesodermal *Bmp4* expression, though comparatively quite weak between E9-10, was detectable early and reduced in $T^{-/-}$ limb buds (Fig. 7I,J). BMP downstream target genes *Msx1* and *Msx2* are expressed throughout ventral ectoderm as well as forming AER, and underlying limb mesoderm (Ahn et al., 2001; Pizette et al., 2001). Despite reduced expression of *Bmp4*, *Msx1* and *Msx2* expression was quantitatively preserved (data not shown), as was BMP target *En1* (below), indicating that the BMP pathway was largely intact.

Pre-AER gene expression and morphology indicated disrupted maturation. *En1* in ventral ectoderm regulates compaction and positioning of mature ventral AER borders by repressing *Wnt7a* (Cygan et al., 1997; Loomis et al., 1998;

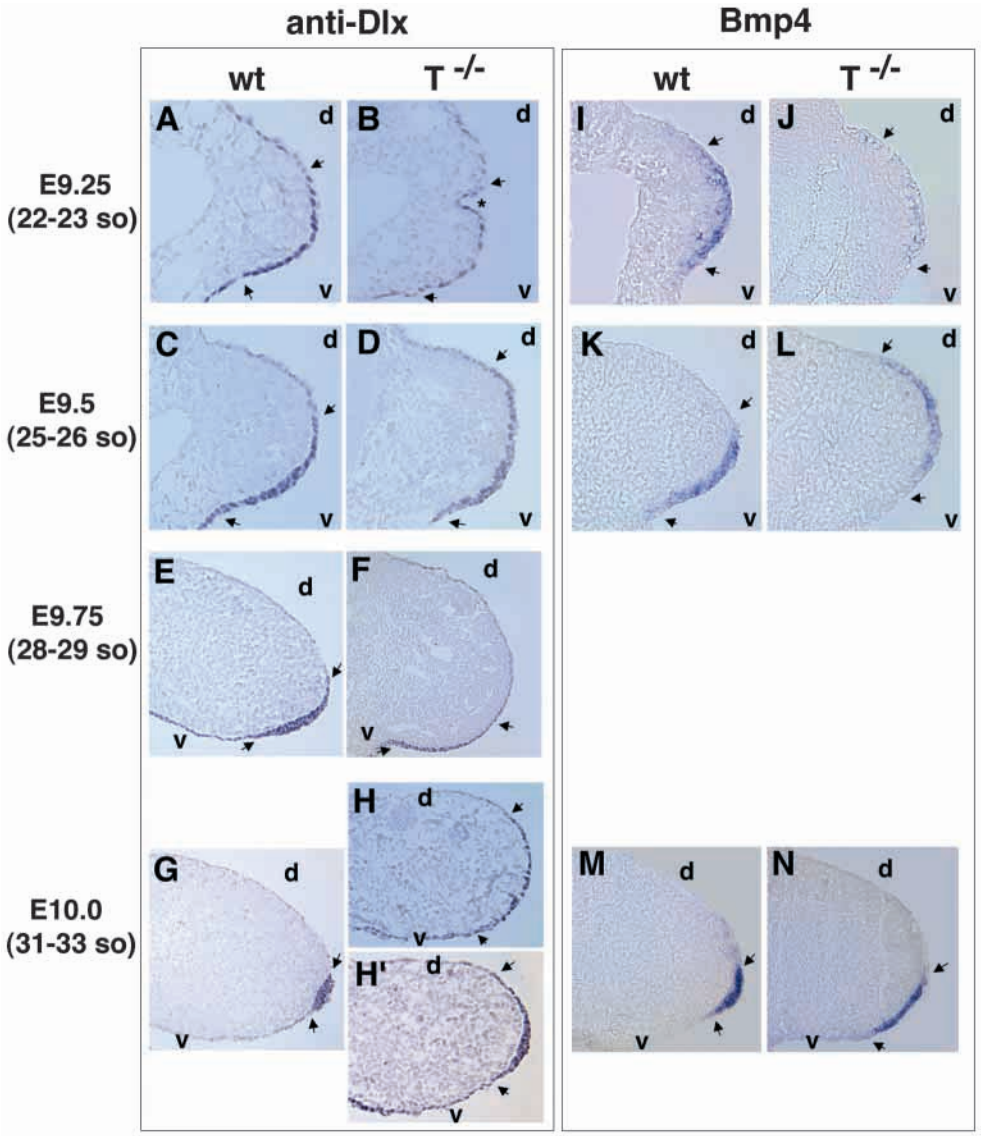

Fig. 7. Abnormal AER morphogenesis in $T^{-/-}$ embryos. AER progenitors were stained with affinity-purified anti-DLX (a gift from Grace Panganiban) in transverse sections of paraffin-embedded wild-type (wt, A,C,E,G) and $T^{-/-}$ (B,D,F,H,H′) forelimb buds at ages (average somite number: so) indicated to the left of the panels. The small arrows indicate approximate extents of pre-AER or AER. Note poor and variable maturation of $T^{-/-}$ AER, as illustrated by H and H′ which show nearby sections from a $T^{-/-}$ limb bud with a particularly mild phenotype. Some $T^{-/-}$ limb buds were highly irregular in shape (* in B; see also Fig. 6Q,T,V). To evaluate distribution of *Bmp4* expression, embryos hybridized in whole-mount were transversely cryo-sectioned and wild type (wt, I,K,M) was compared to $T^{-/-}$ (J,L,N). Similar abnormalities in pre-AER and AER morphology were observed, with poor AER compaction during maturation (eg. M vs.N). Additionally, reduced mesodermal *Bmp4* expression was evident in E9.25 $T^{-/-}$ limb buds (J). d, dorsal; v, ventral.

Kimmel et al., 2000). In $T^{-/-}$ embryos, *Wnt7a* and *En1* were expressed in dorsal and ventral limb bud ectoderm, respectively. However, the distal ectodermal expression borders for each of these genes was not sharp as it is in wild type (Fig. 6K-S), and remained jagged and irregular even at late stages.

Fgf10 induces AER formation and was upregulated by *T* misexpression. *Fgf10* expression declined progressively over time in $T^{-/-}$ embryos compared to wild type (Fig. 6T-X), but did not appear very different until E9.5, after changes in *Fgf8* and *Bmp4* expression were discernible.

Potential late mesenchymal effects of abnormal AER function in $T^{-/-}$ embryos

Proliferation rates, assessed with the mitosis-specific anti-phospho-histone H3 (Gurley et al., 1978), were similar in $T^{-/-}$ and wild-type limb buds at E9.5 and E9.75 (Fig. 8A, and not shown). Normal mitotic rates are not inconsistent with reduced FGF8 in $T^{-/-}$ limb buds; proliferation is unchanged even in *Fgf8*/*Fgf4* nulls despite reduced limb bud size (Sun et al., 2002). Levels of apoptosis, analyzed in sections and whole mount, were similarly very low in wild-type and $T^{-/-}$ limb buds from E9.5-E10 (Fig. 8B, and not shown), even at E10 when extensive apoptosis was present in $T^{-/-}$ axial tissues. Loss of ridge FGF survival signals causes mesenchymal apoptosis, but does not become appreciable until about E10-10.5 (Moon and Capecchi, 2000; Revest et al., 2001; Sun et al., 2002). Thus, abnormalities in $T^{-/-}$ limb buds are not due to general growth arrest and lost viability. They are also unlikely to be due to a general developmental delay. *Lmx1b*, initially expressed uniformly and later restricted to dorsal mesoderm after the AER forms (Loomis et al., 1998), showed normal dorsal restriction in $T^{-/-}$ embryos at E10 (Fig. 8C). However, some mesodermal gene expression was lost. *Shh*, which depends on ridge FGF signals (reviewed by Capdevila and Johnson, 2000), was absent in $T^{-/-}$ limb buds (Fig. 8D). In *Fgfr2-IIIb* null mutants, which fail to form a mature AER, loss of *Shh* induction is evident before other mesodermal changes such as decreased *Msx1*, or increased apoptosis (Revest et al., 2001). The results suggest that *T* plays a role in AER morphogenesis and that altered AER function in $T^{-/-}$ embryos causes some changes in mesodermal gene induction. However, the

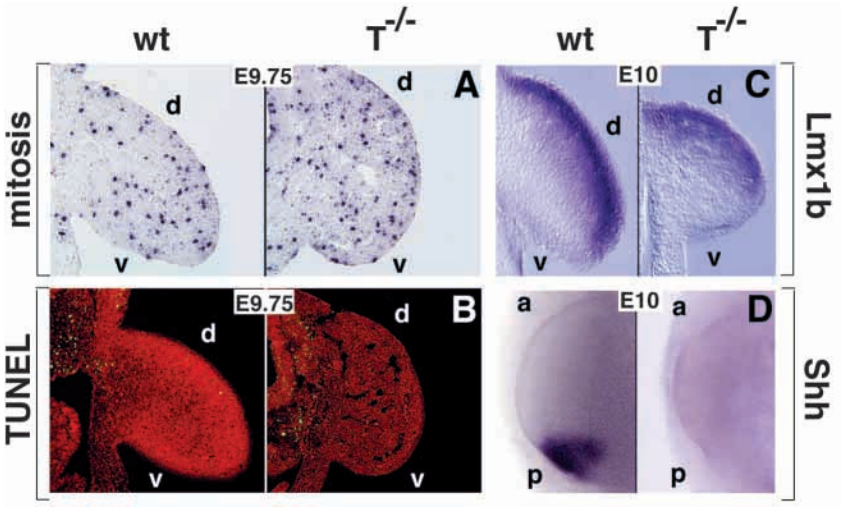

Fig. 8. Selective mesodermal changes consistent with disturbed AER function in $T^{-/-}$ limb buds. Potential changes in limb mesoderm due to altered AER function were evaluated in $T^{-/-}$ embryos (right sides) compared to wild type (wt, left sides). Proliferation was assessed by immunostaining multiple transverse sections with the mitosis-specific anti-phospho-histone H3 (representative sections shown). Similar numbers of mitotic cells were present in wild-type and $T^{-/-}$ limb buds at both E9.5 (not shown) and at E9.75 (A). Apoptosis was evaluated by TUNEL assay at E9.5 (not shown) and E9.75 (B) using fluorescein-UTP (green) and propidium iodide nuclear counterstaining (red) and also by whole-mount Nile Blue sulfate staining at E10 (not shown). At all stages, levels of apoptosis in $T^{-/-}$ limb buds were minimal and similar to wild type. *Lmx1b* and *Shh* were checked to evaluate overall limb 'maturity' and level of AER signaling. *Lmx1b* is expressed uniformly at early stages and dorsally later. *Shh* activation depends on AER signals. While *Lmx1b* expression was preserved and showed nornal dorsal restriction in $T^{-/-}$ limb buds at E10 (C), *Shh* was not expressed at all in $T^{-/-}$ forelimb bud by E10 (D), but was detected at levels similar to wild type in hindgut (data not shown). d, dorsal; v, ventral; a, anterior; p, posterior.

possibility that AER changes in the $T^{-/-}$ embryo are an indirect consequence of lost early midline signals cannot be excluded at present (see Dealy, 1997).

DISCUSSION

T is a well-characterized transcription factor, highly expressed in axial mesoderm and primitive streak, with key roles in mesoderm formation, migration and notochord function (reviewed by Herrmann, 1995). *T* expression has not until now been documented at other sites, presumably because of its very low levels. The timing and pattern of *T* expression in lateral plate and early limb bud suggest a potential role in AER formation. Misexpression in chick prospective limb produced phenotypes consistent with anteriorly extended AER formation and function, while formation of a mature AER compacted towards the DV limb edge was disrupted in $T^{-/-}$ mouse embryos, confirming a role for *T* in AER regulation during normal development.

Restriction of *T* function to the limb apex DV boundary and role in AER maturation

Normal *T* expression in limb bud is restricted to the immediate subridge mesoderm. This may be due to a very stringent dependence of *T* expression on signals from the ridge. In addition to maintenance by ridge signals, lateral inhibitory signals may also serve to limit the zone of *T* expression and/or function. In the ectoderm, *Cux1* is induced along the edges of the forming AER and seems to function to restrict AER formation from spreading laterally (Taveres et al., 2000). Perhaps one of the *Sprouty* genes, which are induced as feedback inhibitors during FGF signaling, could serve a similar role in the limb mesoderm (see Minowada et al., 1999). Even when *T* is uniformly misexpressed throughout the early lateral plate and limb mesoderm, its functional effects are nevertheless restricted to the DV boundary along which AER formation normally occurs, resulting in AER extension along the limb apex. In contrast, certain other factors can induce ectopic AERs in any orientation in limb ectoderm (e.g. Laufer et al., 1997; Rodriguez-Estaban et al., 1997; Kengaku et al., 1998; Pizette et al., 2001). This observed functional restriction could be due to lateral inhibition of *T* function by other limb mesodermal factors. Alternatively, *T* function may require positive mesodermal co-factors that are also restricted to the DV boundary, and so are unavailable to misexpressed *T* elsewhere in the limb. In either case, such restrictions of *T* activity may provide a mesodermal mechanism to ensure that normal AER formation occurs only along the DV boundary in the ectoderm.

The consequences of loss of *T* are also consistent with such a function, and suggest that mesodermal factors may play a role, along with ectodermal factors such as *En1* (Kimmel et al., 2000), in regulating ridge maturation and positioning. However, unlike *En1*, *T* is unlikely to function in AER formation by regulating DV boundary positions. At present, it remains uncertain what mesodermal signal *T* may act through to contribute to AER maturation. At very early stages, BMPs regulate both DV polarity and AER formation in parallel, by inducing *En1* in ventral ectoderm and by activating *Msx* expression, respectively (Ahn et al., 2001; Pizette et al., 2001). Although *Bmp4* expression was reduced early in the $T^{-/-}$ forelimb region, DV polarity was preserved in both ectoderm and mesoderm. Likewise, expression of other BMP targets, *Msx* genes, was unchanged. Consequently, we feel that the BMP signaling pathway is not primarily affected by loss of *T* function; reduced *Bmp4* and irregular *En1* and *Wnt7a* distal expression borders are more likely secondary to some other causative defect in AER morphogenesis. FGF10 plays some role in formation of a mature AER, as well as in limb initiation. In the complete absence of FGF10 no bud or pre-AER forms (Min et al., 1998; Sekine et al., 1999), but loss of the ectodermal FGFR2-IIIb isoform, which FGF10 binds, disrupts AER formation shortly after induction and the expression of *Fgf8* and of early ridge-dependent mesodermal genes is initiated but not maintained (Revest et al., 2001). In $T^{-/-}$ limb buds, *Fgf10* expression is not substantially reduced until E9.5,

but earlier quantitative changes in distal/apical *Fgf10* expression that are difficult to appreciate could still contribute to a hypomorphic effect. However, whether decreased *Fgf10* is directly due to a loss of *T*, or is an indirect effect of reduced AER function cannot be distinguished at present.

Restricted *T* expression along a narrow strip of apical mesoderm could strongly promote AER formation and morphogenesis along the DV boundary by ensuring high focal *Fgf10* expression along the limb apex, or via another mesodermal signal. In the $T^{-/-}$ limb bud, *Fgf8* expression and pre-AER compaction are not properly reinforced along this distal DV border and remain broad and irregular. Alternatively, *T* could play some other role in the mesoderm, such as changing properties of apical mesodermal cells to facilitate compaction of pre-AER ectoderm towards the DV edge.

Potential role of *T* in reciprocal mesenchymal-epithelial signaling in the limb

During limb induction, WNT signals maintain high *Fgf10* expression in prospective limb and FGF10 activates ectodermal *Wnt3a* and *Fgf8* expression, initiating AER formation (Kawakami et al., 2001). AER signals subsequently also maintain mesodermal *Fgf10* expression (Ohuchi et al., 1997). *T* transcripts are first clearly detected at stage 15, at the onset of *Wnt3a* and *Fgf8* activation in the ectoderm (Kengaku et al., 1998). Both the ability of WNT3a and FGF8 to induce *T* expression, and the ability of *T* to increase subridge expression of *Fgf10* early after misexpression suggest that *T* may be a component of the mesodermal response to developing AER signals that maintains high *Fgf10* apically and thereby also maintains the forming AER, establishing a regulatory loop between ectoderm and mesoderm.

The T-box family oversees multiple aspects of limb development

Several T-box genes are expressed in developing limb (Gibson-Brown et al., 1996; Gibson-Brown et al., 1998; Isaac et al., 1998; Logan et al., 1998; Ohuchi et al., 1998), raising the question of specificity of *T* function. *Tbx2* and *Tbx3* are expressed along the anterior and posterior borders of limb mesoderm and in AER as well, but their expression and regulation suggest other than a primary role in AER formation. Both *Tbx2* and *Tbx3* are also expressed in the flank between limb buds and *Tbx3* is down-regulated upon ectopic limb bud induction by FGF (Isaac et al., 1998). Tight regulation of *Tbx3* by SHH (Tumpel et al., 2002) and loss of posterior forelimb elements in humans with *TBX3* mutations [Ulnar-Mammary Syndrome (Bamshad et al., 1997)] both suggest a more direct role for *Tbx3* in AP patterning. *Tbx5* and *Tbx4* are expressed selectively in forelimb or hindlimb mesoderm, respectively, and regulate limb identity (Rodriguez-Esteban et al., 1999; Takeuchi et al., 1999; Bruneau et al., 2001). Loss of *Tbx5* in zebrafish interferes with pectoral fin bud induction and *Tbx5* misexpression in very early chick lateral plate induces ectopic limbs (Ahn et al., 2002; Ng et al., 2002), showing that *Tbx5* also regulates limb outgrowth. However, misexpression of *Tbx5* or *Tbx4* in prospective limb field cause transformations in limb identity and limb truncations (Rodriguez-Esteban et al., 1999; Takeuchi et al., 1999) quite different from *T* misexpression phenotypes. The identities of T-box family targets coordinated throughout limb formation remain to be explored. Because of their different expression patterns and distinct misexpression phenotypes, it is unlikely that *T* and other T-box factors regulate targets redundantly. One interesting possibility is that *T* and *Tbx5* may cooperate in AER regulation, given the dimerization potential of T-box proteins (Muller and Herrmann, 1997). Such dimerization might regulate novel targets, since binding site analyses indicate that different T-box proteins, including T and TBX5, recognize distinct targets in vivo and in vitro (Conlon et al., 2001; Ghosh et al., 2001).

Expression of *T* in relation to several proposed FGF/WNT signal relay sites

Intriguingly, *T* is expressed in association with several sites proposed to 'relay' signals for limb induction from midline to periphery (reviewed by Martin, 1998) including node/early notochord, somites and nephric duct epithelium adjacent to nephrogenic mesoderm. Kawakami et al. (Kawakami et al., 2001) propose that such relay sites may represent points of cross talk for FGF and WNT signals, raising the possibility that *T* plays a role in signal relay at these sites. Such questions are best addressed with genetic approaches, such as a conditionally targeted *T* allele, currently being developed.

We are grateful to Bernard Hermann, Brigid Hogan, Steve Hughes, Alex Joyner, Randy Johnson, Andy McMahon, Richard Maas, Gail Martin, Bruce Morgan, Lee Niswander, Tsutomu Nohno, Sumihare Noji, Dave Ornitz, Bob Riddle and Cliff Tabin for providing plasmids, Grace Panbanigan for the generous gift of affinity purified DLX-antibody, the Genetics Institute for recombinant FGF4 protein, and to Chuxia Deng and Dave Levens for discussions and comments on the manuscript.

REFERENCES

Ahn, K., Mishina, Y., Hanks, M. C., Behringer, R. R. and Crenshaw, E. B. (2001). BMPR-IA signaling is required for the formation of the apical ectodermal ridge and dorsal-ventral patterning of the limb. *Development* **128**, 4449-4461.

Ahn, D. G., Kourakis, M. J., Rohde, L. A., Silver, L. M. and Ho, R. K. (2002). T-box gene Tbx5 is essential for formation of the pectoral limb bud. *Nature* **417**, 754-758.

Altabef, M., Clarke, J. D. W. and Tickle, C. (1997). Dorso-ventral ectodermal compartments and origin of apical ectodermal ridge in developing chick limb. *Development* **124**, 4547-4556.

Arman, E., Haffner-Krausz, R., Gorivodsky, M. and Lona, P. (1999). Fgfr2 is required for limb outgrowth and lung-branching morphogenesis. *Proc. Natl. Acad. Sci. USA* **96**, 11895-11899.

Arnold, S. J., Stappert, J., Bauer, A., Kispert, A., Herrmann, B. G. and Kemler, R. (2000). *Brachyury* is a target gene of the *Wnt/beta-catenin* signaling pathway. *Mech. Dev.* **91**, 249-258.

Bamshad, M., Lin, R. C., Law, D. J., Watkins, W. C., Krakowiak, P. A., Moore, M. E., Franceschini, P., Lala, R., Holmes, L. B., Gebuhr, T. C., Bruneau, B. G., Schinzel, A., Seidman, J. G., Seidman, C. E. and Jorde, L. B. (1997). Mutations in human TBX3 alter limb, apocrine and genital development in ulnar-mammary syndrome. *Nat. Genet.* **16**, 311-315.

Barth, J. and Ivarie, R. (1994). Polyvinyl Alcohol Enhances Detection of Low Abundance Transcripts in Early Stage Quail Embryos in a Nonradioactive Whole Mount In Situ Hybridization Technique. *BioTechniques* **17**, 324-327.

Bruneau, B. G., Nemer, G., Schmitt, J. P., Charron, F., Robitaille, L., Caron, S., Conner, D. A., Gessler, M., Nemer, M., Seidman, C. E. and Seidman, J. G. (2001). A murine model of Holt-Oram syndrome defines roles of the T-box transcription factor *Tbx5* in cardiogenesis and disease. *Cell* **106**, 709-721.

Capdevila, J. and Johnson, R. L. (2000). *Hedgehog* signaling in vertebrate and invertebrate limb patterning. *Cell. Mol. Life Sci.* **57**, 1682-1694.

Chen, H., Lun, Y., Ovchinnikov, D., Kokubo, H., Oberg, K. C., Pepicelli, C. V., Gan, L., Lee, B. and Johnson, R. L. (1998). Limb and kidney defects in *Lmx1b* mutant mice suggest an involvement of LMX1B in human nail patella syndrome. *Nat. Genet.* **1**, 51-55.

Cohn, M. J., Izpisúa-Belmonte, J. C., Abud, H., Heath, J. K. and Tickle, C. (1995). Fibroblast growth factors induce additional limb development from the flank of chick embryos. *Cell* **80**, 739-746.

Conlon, F. L., Fairclough, L., Price, B. M., Casey, E. S. and Smith, J. C. (2001). Determinants of T-box protein specificity. *Development* **128**, 3749-3758.

Crossley, P. H., Minowada, G., MacArthur, C. A. and Martin, G. R. (1996). Roles for FGF8 in the induction, initiation, and maintenance of chick limb development. *Cell* **84**, 127-136.

Cygan, J. A., Johnson, R. L. and McMahon, A. P. (1997). Novel regulatory interactions revealed by studies of murine limb pattern in Wnt-7a and En-1 mutants. *Development* **124**, 5021-5032.

Dealy, C. N. (1997). Hensen's node provides an endogenous limb-forming signal. *Dev. Biol.* **188**, 216-223.

Galceran, J., Hsu, S. C. and Grosschedl, R. (2001). Rescue of a *Wnt* mutation by an activated form of LEF 1: regulation of maintenance but not initiation of *Brachyury* expression. *Proc. Natl. Acad. Sci. USA* **98**, 8668-8673.

Galceran, J., Farinas, I., Depew, M. J., Clevers, H. and Grosschedl, R. (1999). *Wnt3a*$^{-/-}$ like phenotype and limb deficiency in *Lef1*$^{-/-}$*Tcf1*$^{-/-}$ mice. *Genes Dev.* **13**, 709-717.

Ghosh, T. K., Packham, E. A., Bonser, A. J., Robinson, T. E., Cross, S. J. and Brook, J. D. (2001). Characterization of the TBX5 binding site and analysis of mutations that cause Holt-Oram syndrome. *Hum. Mol. Genet.* **10**, 1983-1994.

Gibson-Brown, J. J., Agulnik, S. I., Chapman, D. L., Alexiou, M., Garvey, N., Silver, L. M. and Papaioannou, V. E. (1996). Evidence of a role for T-box genes in the evolution of limb morphogenesis and the specification of forelimb/hindlimb identity. *Mech. Dev.* **56**, 93-101.

Gibson-Brown, J. J., Agulnik, S. I., Silver, L. M., Niswander, L. and Papaioannou, V. E. (1998). Involvement of T-box genes *Tbx2-Tbx5* in vertebrate limb specification and development. *Development* **125**, 2499-2509.

Gurley, L. R., D'Anna, J. A., Barham, S. S., Deaven, L. L. and Tobey, R. A. (1978). Histone phosphorylation and chromatin structure during mitosis in Chinese hamster cells. *Eur. J. Biochem.* **84**, 1-15.

Hamburger, V. and Hamilton, H. L. (1951). A series of normal stages in the development of the chick. *J. Morphol.* **8**, 49-92.

Haramis, A. G., Brown, J. M. and Zeller, R. (1995). The limb deformity mutation disrupts the SHH/FGF-4 feedback loop and regulation of 5′ *HoxD* genes during limb pattern formation. *Development* **121**, 4237-4245.

Herrmann, B. G. (1995). The mouse *Brachyury* (*T*). gene. *Sem. Dev. Biol.* **6**, 385-394.

Herrmann, B. G., Labeit, S., Poustka, A., King, T. R. and Lehrach, H. (1990). Cloning of the *T* gene required in mesoderm formation in the mouse. *Nature* **343**, 617-622.

Isaac, A., Rodriguez-Esteban, C., Ryan, A., Altabef, M., Tsukui, T., Patel, K., Tickle, C. and Izpisua-Belmonte, J. C. (1998). *Tbx* genes and limb identity in chick embryo development. *Development* **125**, 1867-1875.

Kawakami, Y., Capdevila, J., Buscher, D., Itoh, T., Rodriguez Esteban, C. and Izpisua-Belmonte, J. C. (2001). WNT signals control FGF-dependent limb initiation and AER induction in the chick embryo. *Cell* **104**, 891-900.

Kengaku, M., Capdevila, J., Rodriguez-Esteban, C., De La Pena, J., Johnson, R. L., Belmonte, J. C. I. and Tabin, C. J. (1998). Distinct WNT pathways regulating AER formation and dorsoventral polarity in the chick limb bud. *Science* **280**, 1274-1277.

Kimmel, R. A., Turnbull, D. H., Blanquet, V., Wurst, W., Loomis, C. A. and Joyner, A. L. (2000). Two lineage boundaries coordinate vertebrate apical ectodermal ridge formation. *Genes Dev.* **14**, 1377-1389.

Kimura, J., Sato-Maeda, M., Noji, S. and Ide, H. (2000). Synergistic effects of FGF and non-ridge ectoderm on gene expression involved in the formation of the anteroposterior axis of the chick limb bud in cell culture. *Dev. Growth Differ.* **42**, 219-227.

Kispert, A. and Herrmann, B. G. (1993). The *Brachyury* gene encodes a novel DNA binding protein. *EMBO J.* **12**, 3211-3220.

Knezevic, V., de Santo, R. and Mackem, S. (1997a). Two novel chick T-box genes related to mouse *Brachyury* are expressed in different, non-overlapping mesoderal domains during gastrulation. *Development* **124**, 411-419.

Knezevic, V., De Santo, R., Schughart, K., Huffstadt, U., Chiang, C., Mahon, K. and Mackem, S. (1997b). *Hoxd-12* differentially affects preaxial and postaxial chondrogenic branches in the limb and regulates Sonic hedgehog in a positive feedback loop. *Development* **124**, 4523-4536.

Laufer, E., Dahn, R., Orozco, O. E., Yeo, C. Y., Pisenti, J., Henrique, D., Abbott, U. K., Fallon, J. F. and Tabin, C. (1997). Expression of radical fringe in limb-bud ectoderm regulates apical ectodermal ridge formation. *Nature* **386**, 366-373.

Lewandoski, M., Sun, X. and Martin, G. R. (2000). *Fgf8* signalling from the AER is essential for normal limb development. *Nat, Genet.* **26**, 460-463.

Lewis, P. M., Dunn, M. P., McMahon, J. A., Logan, M., Martin, J. F., St-Jacques, B. and McMahon, A. P. (2001). Cholesterol modification of *sonic hedgehog* is required for long-range signaling activity and effective modulation of signaling by *Ptc1*. *Cell* **105**, 599-612.

Logan, C., Hornbruch, A., Campbell, I. and Lumsden, A. (1997). The role of *Engrailed* in establishing the dorsoventral axis of the chick limb. *Development* **124**, 2317-2324.

Logan, M., Simon, H. G. and Tabin, C. (1998). Differential regulation of T-box and homeobox transcription factors suggests roles in controlling chick limb-type identity. *Development* **125**, 2825-2835.

Loomis, C. A., Harris, E., Michaud, J., Wurst, W., Hanks, M. and Joyner, A. L. (1996). The mouse *Engrailed-1* gene and ventral limb patterning. *Nature* **382**, 360-363.

Loomis, C. A., Kimmel, R. A., Tong, C. X., Michaud, J. and Joyner, A. L. (1998). Analysis of the genetic pathway leading to formation of ectopic apical ectodermal ridges in mouse *Engrailed-1* mutant limbs. *Development* **125**, 1137-1148.

Mahmood, R., Bresnick, J., Hornbruch, A., Mahony, C., Morton, N., Colquhoun, K., Martin, P., Lumsden, A., Dickson, C. and Mason, I. (1995). A role for FGF-8 in the initiation and maintenance of vertebrate limb bud outgrowth. *Curr Biol.* **5**, 797-806.

Martin, G. R. (1998). The roles of FGFs in the early development of vertebrate limbs. *Genes Dev.* **12**, 1571-1586.

Michaud, J. L., Lapointe, F. and LeDouarin, N. M. (1997). The dorsoventral polarity of the presumptive limb is determined by signals produced by the somites and by the lateral somatopleure. *Development* **124**, 1453-1463.

Min, H. S., Danilenko, D. M., Scully, S. A., Bolon, B., Ring, B. D., Tarpley, J. E., DeRose, M. and Simonet, W. S. (1998). *Fgf-10* is required for both limb and lung development and exhibits striking functional similarity to *Drosophila branchless*. *Gene Dev.* **12**, 3156-3161.

Minowada, G., Jarvis, L. A., Chi, C. L., Neubuser, A., Sun, X., Hacohen, N., Krasnow, M. A. and Martin, G. R. (1999). Vertebrate *Sprouty* genes are induced by FGF signaling and can cause chondrodysplasia when overexpressed. *Development* **126**, 4465-4475.

Moon, A. M. and Capecchi, M. R. (2000). *Fgf8* is required for outgrowth and patterning of the limbs. *Nat. Genet.* **26**, 455-459.

Morgan, B. A. and Fekete, D. M. (1996). Manipulating gene expression with replication-competent retroviruses. *Method Cell Biol.* **51**, 185-218.

Muller, C. W. and Herrmann, B. G. (1997). Crystallographic structure of the T domain DNA complex of the Brachyury transcription factor. *Nature* **389**, 884-888.

Ng, J. K., Kawakami, Y., Büscher, D., Raya, A., Itoh, T., Koth, C. M., Rodríguez-Esteban, C., Rodríguez-León, J., Garrity, D. M., Fishman, M. C. and Izpisúa-Belmonte, J. C. (2002). The limb identity gene Tbx5 promotes limb initiation by interacting with Wnt2b and Fgf10. *Development* **129**, 5161-5170.

Ohuchi, H., Nakagawa, T., Yamamoto, A., Araga, A., Ohata, T., Ishimaru, Y., Yoshioka, H., Kuwana, T., Nohno, T., Yamasaki, M., Itoh, N. and Noji, S. (1997). The mesenchymal factor, *Fgf10*, initiates and maintains the outgrowth of the chick limb bud through interaction with FGF8, an apical ectodermal factor. *Development* **124**, 2235-2244.

Ohuchi, H., Takeuchi, J., Yoshioka, H., Ishimaru, Y., Ogura, K., Takahashi, N., Ogura, T. and Noji, S. (1998). Correlation of wing-leg identity in ectopic FGF-induced chimeric limbs with the differential expression of chick *Tbx5* and *Tbx4*. *Development* **125**, 51-60.

Ornitz, D. M., Xu, J., Colvin, J. S., McEwen, D. G., MacArthur, C. A., Coulier, F., Gao, G. and Goldfarb, M. (1996). Receptor specificity of the fibroblast growth factor family. *J. Biol. Chem.* **271**, 15292-15297.

Panganiban, G., Irvine, S. M., Lowe, C., Roehl, H., Corley, L. S., Sherbon, B., Grenier, J. K., Fallon, J. F., Kimble, J., Walker, M., Wray, G. A., Swalla, B. J., Martindale, M. Q. and Carroll, S. B. (1997). The origin and evolution of animal appendages. *Proc. Natl. Acad. Sci. USA* **94**, 5162-5166.

Papaioannou, V. E. and Silver, L. M. (1998). The T-box gene family. *BioEssays* **20**, 9-19.

Parr, B. A. and McMahon, A. P. (1995). Dorsalizing signal *Wnt-7a* required for normal polarity of D-V and A-P axes of mouse limb. *Nature* **374**, 350-353.

Pizette, S. and Niswander, L. (1999). BMPs negatively regulate structure and function of the limb apical ectodermal ridge. *Development* **126**, 883-894.

Pizette, S., Abate-Shen, C. and Niswander, L. (2001). BMP controls proximodistal outgrowth, via induction of the apical ectodermal ridge, and dorsoventral patterning in the vertebrate limb. *Development* **128**, 4463-4474.

Revest, J. M., Spencer-Dene, B., Kerr, K., De Moerlooze, L., Rosewell, I. and Dickson, C. (2001). Fibroblast growth factor receptor 2-IIIb acts upstream of Shh and Fgf4 and is required for limb bud maintenance but not for the induction of Fgf8, Fgf10, Msx1| or Bmp4. *Dev. Biol.* **231**, 47-62.

Riddle, R. D., Ensini, M., Nelson, C., Tsuchida, T., Jessell, T. M. and Tabin, C. (1995). Induction of the LIM homeobox gene *Lmx1* by WNT7a establishes dorsoventral pattern in the vertebrate limb. *Cell* **83**, 631-640.

Rodriguez-Esteban, C., Schwabe, J. W. R., DeLaPena, J., Foys, B., Eshelman, B. and Izpisua-Belmonte, J. C. (1997). Radical fringe positions the apical ectodermal ridge at the dorsoventral boundary of the vertebrate limb. *Nature* **386**, 360-366.

Rodriguez-Esteban, C., Tsukui, T., Yonei, S., Magallon, J., Tamura, K. and Izpisua Belmonte, J. C. (1999). The T-box genes *Tbx4* and *Tbx5* regulate limb outgrowth and identity. *Nature* **398**, 814-818.

Sekine, K., Ohuchi, H., Fujiwara, M., Yamasaki, M., Yoshizawa, T., Sato, T., Yagishita, N., Matsui, D., Koga, Y., Itoh, N. and Kato, S. (1999). *Fgf10* is essential for limb and lung formation. *Nat. Genet.* **21**, 138-141.

Smith, J. C., Armes, N. A., Conlon, F. L., Tada, M., Umbhauer, M. and Weston, K. M. (1997). Upstream and downstream from *Brachyury*, a gene required for vertebrate mesoderm formation. *Cod Spring Harb. Symp. Quant. Biol.* **62**, 337-346.

Sun, X., Mariani, F. V. and Martin, G. R. (2002). Functions of FGF signalling from the apical ectodermal ridge in limb development. *Nature* **418**, 501-508.

Tada, M. and Smith, J. C. (2000). *Xwnt11* is a target of *Xenopus Brachyury*: regulation of gastrulation movements via *Dishevelled*, but not through the canonical *Wnt* pathway. *Development* **127**, 2227-2238.

Takeuchi, J. K., Koshiba-Takeuchi, K., Matsumoto, K., Vogel-Hopker, A., Naitoh-Matsuo, M., Ogura, K., Takahashi, N., Yasuda, K. and Ogura, T. (1999). *Tbx5* and *Tbx4* genes determine the wing/leg identity of limb buds. *Nature* **398**, 810-814.

Tavares, A. T., Tsukui, T. and Izpisua-Belmonte, J. C. (2000). Evidence that members of the *Cut/Cux/CDP* family may be involved in AER positioning and polarizing activity during chick limb development. *Development* **127**, 5133-5144.

Tickle, C. and Munsterberg, A. (2001). Vertebrate limb development: the early stages in chick and mouse. *Curr. Opin. Genet. Dev*. **11**, 476-481.

Tumpel, S., Sanz-Ezquerro, J. J., Isaac, A., Eblaghie, M. C., Dobson, J. and Tickle, C. (2002). Regulation of Tbx3 expression by anteroposterior signalling in vertebrate limb development. *Dev. Biol.* **250**, 251-262.

Vogel, A., Rodriguez, C., Warnken, W. and Izpisua-Belmonte, J. C. (1995). Dorsal cell fate specified by chick *Lmx1* during vertebrate limb development. *Nature* **378**, 716-720.

Xu, X. L., Weinstein, M., Li, C. L., Naski, M., Cohen, R. I., Ornitz, D. M., Leder, P. and Deng, C. X. (1998). Fibroblast growth factor receptor 2 (FGFR2)-mediated reciprocal regulation loop between FGF8 and FGF10 is essential for limb induction. *Development* **125**, 753-765.

Yamaguchi, T. P., Takada, S., Yoshikawa, Y., Wu, N. and McMahon, A. P. (1999a). *T* (*Brachyury*) is a direct target of *Wnt3a* during paraxial mesoderm specification. *Genes Dev.* **13**, 3185-3190.

Yamaguchi, T. P., Bradley, A., McMahon, A. P. and Jones, S. A. (1999b). *Wnt5a* pathway underlies outgrowth of multiple structures in the vertebrate embryo. *Development* **126**, 1211-1223.

Zeller, R. and Duboule, D. (1997). Dorso-ventral limb polarity and origin of the ridge: on the fringe of independence? *BioEssays* **19**, 541-546.

Zhang, Z., Yu, X., Zhang, Y., Geronimo, B., Lovlie, A., Fromm, S. H. and Chen, Y. (2000). Targeted misexpression of constitutively active BMP receptor-IB causes bifurcation, duplication, and posterior transformation of digit in mouse limb. *Dev. Biol.* **220**, 2154-2167.